

Supersymmetry production cross sections in pp collisions at $\sqrt{s} = 7$ TeV

Michael Krämer

Institut für Theoretische Teilchenphysik und Kosmologie, RWTH Aachen, Germany

Anna Kulesza

Institut für Theoretische Physik, Westfälische Wilhelms-Universität Münster, D-48149 Münster, Germany

Robin van der Leeuw

Nikhef National Institute for Subatomic Physics and University of Amsterdam, Amsterdam, Netherlands

Michelangelo Mangano

European Organization for Nuclear Research, CERN, Switzerland

Sanjay Padhi

University of California, San Diego, USA

Tilman Plehn

Institut für Theoretische Physik, Universität Heidelberg, Germany

Xavier Portell

European Organization for Nuclear Research, CERN, Switzerland

Abstract

This document emerged from work that started in January 2012 as a joint effort by the ATLAS, CMS and LPCC supersymmetry (SUSY) working groups to compile state-of-the-art cross section predictions for SUSY particle production at the LHC. We present cross sections for various SUSY processes in pp collisions at $\sqrt{s} = 7$ TeV, including an estimate of the theoretical uncertainty due to scale variation and the parton distribution functions. Further results for higher LHC centre-of-mass energies will be collected at <https://twiki.cern.ch/twiki/bin/view/LHCPhysics/SUSYCrossSections>. For squark and gluino production, which dominate the inclusive SUSY cross section, we employ calculations which include the resummation of soft gluon emission at next-to-leading logarithmic accuracy, matched to next-to-leading order (NLO) SUSY-QCD. In all other cases we rely on NLO SUSY-QCD predictions.

1 Introduction

The search for supersymmetry (SUSY) is a central activity of the LHC physics programme. In the framework of the Minimal Supersymmetric extension of the Standard Model (MSSM) with R-parity conservation, SUSY particles are pair produced. At the LHC, the most copiously produced SUSY particles are expected to be the strongly interacting partners of quarks, the squarks (\tilde{q}), and the partners of gluons, the gluinos (\tilde{g}). The squark and gluino pair-production processes to be considered are

$$pp \rightarrow \tilde{q}\tilde{q}, \tilde{q}\tilde{q}^*, \tilde{q}\tilde{g}, \tilde{g}\tilde{g} + X, \quad (1)$$

together with the charge conjugated processes. In Eq. (1) the chiralities of the squarks, $\tilde{q} = (\tilde{q}_L, \tilde{q}_R)$, are suppressed, and we focus on the production of the partners of the (u, d, c, s, b) quarks which we assume to be mass-degenerate. The production of the SUSY partners of top quarks, the stops (\tilde{t}), and, when appropriate, the partners of bottom quarks, the sbottoms (\tilde{b}), has to be considered separately due to parton distribution function (PDF) effects and potentially large mixing affecting the mass splittings. In this case, we explicitly specify the different mass states in the pair-production processes,

$$pp \rightarrow \tilde{t}_i\tilde{t}_i^*, \tilde{b}_i\tilde{b}_i^* + X \quad i = 1, 2, \quad (2)$$

where $i = 1, 2$ corresponds to the lighter and heavier states, respectively. Furthermore, if weak-scale SUSY is realised in nature, the production of SUSY partners of the electroweak particles in the Standard Model, namely the gauginos and higgsinos, need also to be considered.

A comprehensive search program sensitive to the production of SUSY particles has been underway at the LHC, since the beginning of the data-taking process. These searches aim for a broad range of possible final states [1, 2]. Given the importance of SUSY searches at the LHC, accurate knowledge of theoretical predictions for the cross sections is required. The interpretation, in terms of exclusion limits, of the results from the Tevatron, the 2010 LHC data and the first set of the 2011 LHC events, used next-to-leading order (NLO) predictions. However, over the past few years, substantial progress has been made in calculating higher-order corrections for squark and gluino production cross sections. In particular, the resummed results at the next-to-leading logarithmic (NLL) accuracy matched to NLO predictions have become available, allowing for a significant reduction of the theoretical uncertainties related to unknown higher perturbative orders. Therefore, it is desirable to implement this recent progress in the forthcoming set of analyses of the most recent LHC data sets. In the case of electroweak or strong-weak production, i.e. production processes in which sleptons and gauginos are involved, the NLO predictions are used.

This document emerged from discussions among the SUSY working groups of ATLAS, CMS and of the LHC physics center at CERN (LPCC) [3]. The aim is to provide a reference for the collaborations on the evaluation of the production cross sections and their associated uncertainties, along the lines of similar recommendations developed by the PDF4LHC [4] forum and by the Higgs cross section working group [5, 6]. For the purpose of illustration, this document will present some explicit results for $\sqrt{s} = 7$ TeV. The detailed cross section values for the relevant processes and SUSY models considered by the experiments, as well as the results for higher LHC centre-of-mass energies, will be collected at the SUSY cross section working group twiki page [7].

The next section briefly describes the current state-of-the-art higher order calculations, followed by the prescription used for the treatment of theoretical uncertainties in section 3. In sections 4 and 5, the production cross sections for coloured SUSY states and electroweak SUSY productions are shown, respectively. A summary of the results and of the future prospects is given in section 6.

2 Higher order calculations – NLO+NLL

The dependence of hadron collider observables on the renormalisation and factorisation scales is an artifact of perturbation theory. This is typically reduced as higher-order perturbative contributions are included. Assuming that there is no systematic shift of an observable from order to order in perturbation theory, for example due to the appearance of new production channels, the range of rates covered by the scale dependence at a given loop order should include the true prediction of this rate. The scale dependence gives us therefore a lower limit on the theory uncertainty of a QCD prediction, which becomes smaller as higher-order SUSY-QCD corrections are included. To estimate the scale uncertainty in this study we vary simultaneously factorisation and renormalisation scales, within a range of 0.5 to 2 times the reference central scale μ , where μ is the average of the two sparticle masses in the final state. In the future, we shall study the effect of varying renormalisation and factorisation scales independently.

The corrections often increase the size of the cross section with respect to the leading-order prediction [8, 9, 10] if the renormalisation and factorisation scales are chosen close to the average mass of the produced SUSY particles. As a result, the SUSY-QCD corrections have a substantial impact on the determination of mass exclusion limits and would lead to a significant reduction of uncertainties on SUSY mass or parameter values in the case of discovery, see e.g. [11]. The processes listed in Eqs. (1) and (2) have been known for quite some time at NLO in SUSY-QCD [12, 13, 14, 15]. Note that SUSY-QCD corrections can be split into two parts: first, the QCD corrections induced by gluon or quark radiation and by gluon loops, which follow essentially the same pattern as, for example, the top pair production, and second, the virtual diagrams which involve squark and gluino loops, which are independent of the real emission corrections. For relatively heavy SUSY spectra the latter are numerically sub-leading terms which are, however, challenging to compute. This is mainly due to a large number of Feynman diagrams with many different mass scales contributing to the overall cross section. For example for stop pair production, where neither light-flavour squarks nor gluinos appear in the tree-level diagrams, these contributions can be easily decoupled [15]. The only part which requires some attention is the appropriate treatment of the counter term and the running of the strong coupling constant. This decoupling limit is implemented in PROSPINO2 [16]. For light-flavour squark and gluino production this decoupling would only be consistent if applied to the leading order as well as NLO contributions. This is usually not required, unless we choose specific simplified models.

Given the expected squark flavour structure in the MSSM, most numerical implementations, including PROSPINO2, make assumptions about the squark mass spectrum. The left-handed and right-handed squarks of the five light flavours are assumed to be mass degenerate. Only the two stop masses are kept separate in the NLO computations of light-flavour production rates [12, 13, 14]. In the PROSPINO2 [16] implementation, this degeneracy is not assumed for the leading-order results. However, the approximate NLO rates are computed from the exact leading order cross sections times the mass degenerate K factors. For the pair production of third-generation squarks the four light squark flavours are mass degenerate, while the third generation masses are kept separate [15]. This approximation can for example be tested using MADGOLEM [17], an automated NLO tool linked to MADGRAPH4 [18]. It is also important to point out here that in PROSPINO2 the pair production of third-generation squarks is available as individual processes. However, sbottom pairs are included in the implicit sum of light-flavour squarks because there is no perfect separation of bottom and light-flavour decay jets.

When summing the squark and gluino production rates including next-to-leading order corrections it is crucial to avoid double counting of processes. For example, squark pair production includes $\mathcal{O}(\alpha_s^3)$ processes of the kind $gg \rightarrow \tilde{q}\tilde{q}^*q$. The same final state can be produced in $\tilde{q}\tilde{g}$ production when the on-shell gluino decays into an anti-squark and a quark. The PROSPINO scheme for the separation and subtraction of on-shell divergences from the $\tilde{q}\tilde{q}^*$ process uniquely ensures a consistent and point-by-point separation over the entire phase space. For a finite particle mass it has recently been adopted by MC@NLO [19] for top quark processes. It is automated as part of MADGOLEM [17].

A significant part of the NLO QCD corrections can be attributed to the threshold region, where the partonic centre-of-mass energy is close to the kinematic production threshold. In this case the NLO corrections are typically large, with the most significant contributions coming from soft-gluon emission off the coloured particles in the initial and final state. The contributions due to soft gluon emission can be consistently taken into account to all orders by means of threshold resummation. In this paper, we discuss results where resummation has been performed at next-to-leading logarithmic (NLL) accuracy [20, 21, 22, 23, 24].

The step from NLO to NLO+NLL is achieved by calculating the NLL-resummed partonic cross section $\tilde{\sigma}^{(\text{NLL})}$ and then matching it to the NLO prediction, in order to retain the available information on other than soft-gluon contributions. The matching procedure takes the following form

$$\begin{aligned} \sigma_{pp \rightarrow kl}^{(\text{NLO+NLL})}(\rho, \{m^2\}, \mu^2) &= \sigma_{pp \rightarrow kl}^{(\text{NLO})}(\rho, \{m^2\}, \mu^2) \\ &+ \frac{1}{2\pi i} \sum_{i,j=q,\bar{q},g} \int_{\text{CT}} dN \rho^{-N} \tilde{f}_{i/p}(N+1, \mu^2) \tilde{f}_{j/p}(N+1, \mu^2) \\ &\times \left[\tilde{\sigma}_{ij \rightarrow kl}^{(\text{NLL})}(N, \{m^2\}, \mu^2) - \tilde{\sigma}_{ij \rightarrow kl}^{(\text{NLL})}(N, \{m^2\}, \mu^2)|_{(\text{NLO})} \right], \end{aligned} \quad (3)$$

where the last term in the square brackets denotes the NLL resummed expression expanded to NLO. The symbol $\{m^2\}$ stands for all masses entering the calculations and μ is the common factorisation and renormalisation scale. The resummation is performed in the Mellin moment N space, with all Mellin-transformed quantities indicated by

tilde. In particular, the Mellin moments of the partonic cross sections are defined as

$$\tilde{\sigma}_{ij \rightarrow kl}(N, \{m^2\}, \mu^2) \equiv \int_0^1 d\hat{\rho} \hat{\rho}^{N-1} \sigma_{ij \rightarrow kl}(\hat{\rho}, \{m^2\}, \mu^2). \quad (4)$$

The variable $\hat{\rho} \equiv (m_k + m_l)^2/\hat{s}$ measures the closeness to the partonic production threshold and is related to the corresponding hadronic variable $\rho = \hat{\rho}x_i x_j$ in Eq. (3), where x_i (x_j) are the usual longitudinal momentum fraction of the incoming proton carried out by the parton i (j). The necessary inverse Mellin transform in Eq. (3) is performed along the contour CT according to the so-called ‘‘minimal prescription’’ [25]. The NLL resummed cross section in Eq. (3) reads

$$\begin{aligned} \tilde{\sigma}_{ij \rightarrow kl}^{(\text{NLL})}(N, \{m^2\}, \mu^2) &= \sum_I \tilde{\sigma}_{ij \rightarrow kl, I}^{(0)}(N, \{m^2\}, \mu^2) \\ &\times \Delta_i^{(\text{NLL})}(N+1, Q^2, \mu^2) \Delta_j^{(\text{NLL})}(N+1, Q^2, \mu^2) \Delta_{ij \rightarrow kl, I}^{(\text{s, NLL})}(N+1, Q^2, \mu^2), \end{aligned} \quad (5)$$

where the hard scale Q^2 is taken as $Q^2 = (m_k + m_l)^2$ and $\tilde{\sigma}_{ij \rightarrow kl, I}^{(0)}$ are the colour-decomposed leading-order cross sections in Mellin-moment space, with I labelling the possible colour structures. The functions $\Delta_i^{(\text{NLL})}$ and $\Delta_j^{(\text{NLL})}$ sum the effects of the (soft-)collinear radiation from the incoming partons. They are process-independent and do not depend on the colour structures. These functions contain both the leading logarithmic as well as part of the sub-leading logarithmic behaviour. The expressions for $\Delta_i^{(\text{NLL})}$ and $\Delta_j^{(\text{NLL})}$ can be found in the literature [21]. In order to perform resummation at NLL accuracy, one also has to take into account soft-gluon contributions involving emissions from the final state, depending on the colour structures in which the final state SUSY particle pairs can be produced. They are summarised by the factor

$$\Delta_I^{(\text{s, NLL})}(N, Q^2, \mu^2) = \exp \left[\int_{\mu}^{Q/N} \frac{dq}{q} \frac{\alpha_s(q)}{\pi} D_I \right]. \quad (6)$$

The one-loop coefficients D_I follow from the threshold limit of the one-loop soft anomalous-dimension matrix and can be found in [21, 22].

The analytic results for the NLL part of the cross sections have been implemented into a numerical code. The results of this code, added to the NLO results obtained from PROSPINO2, correspond to the matched NLO+NLL cross sections. Their central values, the scale uncertainty and the 68% C.L. pdf and α_s uncertainties obtained using CTEQ6.6 [26] and MSTW2008 [27] PDFs have been tabulated for the squark and gluino production processes of interest in the range of input masses appropriate for the current experimental analysis.¹⁾ The set of tabulated values has enough granularity in order to minimise the interpolation uncertainty when an intermediate value is used as input in the analysis. Together with a corresponding interpolation code, the tabulated values constitute the NLL-FAST numerical package [24, 29].

Note that for specific processes, results beyond NLL accuracy are already available. The production of squark-antisquark pairs has been calculated at next-to-next-to-leading-logarithmic (NNLL) level [30]. Also, a general formalism has been developed in the framework of effective field theories which allows for the resummation of soft and Coulomb gluons in the production of coloured sparticles [31, 32] and subsequently applied to squark and gluino production [32, 33]. In addition, the dominant next-to-next-to-leading order (NNLO) corrections, including those coming from the resummed cross section at next-to-next-to-leading-logarithmic (NNLL) level, have been calculated for squark-antisquark pair-production [34, 35]. The production of gluino bound states as well as bound-state effects in gluino-pair and squark-gluino production has also been studied [36, 37, 38, 39]. Furthermore, electroweak corrections to the $\mathcal{O}(\alpha_s^2)$ tree-level processes [40, 41, 42, 43, 44, 45, 46] and the electroweak Born production channels of $\mathcal{O}(\alpha\alpha_s)$ and $\mathcal{O}(\alpha^2)$ [47, 48] are in general significant for the pair production of SU(2)-doublet squarks \tilde{q}_L and at large invariant masses, but they are moderate for inclusive cross sections and will not be included in the results presented here.

¹⁾ Note that we use NLO pdfs with the NLO+NLL matched cross section calculation. The reduction of the factorisation scale dependence observed in the NLO+NLL predictions is a result of a better compensation between the scale dependence of the NLO evolution of the pdf and the short distance cross section, and does not depend on whether pdfs are fitted using NLO or NLO+NLL theory, see for example Ref. [28]. In general, one can apply NLL threshold resummation with NLO pdfs to processes like heavy SUSY particle production for which the summation of logarithms is more important than for the input data to the NLO fits. However, it would be interesting to systematically study the difference between NLO and NLO+NLL input to global pdf determinations for SUSY particle production at the LHC.

Resummation has also been studied for the production of electroweak SUSY particles, see Refs. [49, 50, 51, 52, 53, 54, 55, 56]. However, since the electroweak processes do not significantly contribute to the inclusive SUSY cross section in general, we use the NLO-SUSY QCD calculation [57, 58, 59] for their evaluation.

3 Treatment of cross sections and their associated uncertainties

Here, the determination of the cross section central values and associated systematic uncertainties is discussed in detail, in view of the recent progress discussed in the previous section.

In case of pair production processes of strongly interacting particles, for which NLL calculations exist, the cross sections are taken at the next-to-leading order in the strong coupling constant, including the resummation of soft gluon emission at the NLL level of accuracy, performed using the NLL-FAST code.

These cross sections are currently available for masses spanning 200 GeV to 2 TeV for squarks and gluinos and 100 GeV to 1 TeV for direct stop or sbottom pair production. In the case of associated squark-gluino production and gluino-pair production processes, the calculations are extended up to squark masses of 3.5 TeV and 4.5 TeV, respectively. Following the convention used in PROSPINO2, in the case of squarks, which can be more or less degenerate depending on a specific SUSY scenario, the input mass used is the result of averaging only the first and second generation squark masses. Further details on different scenarios considered to interpret the variety of experimental searches developed by the ATLAS and CMS collaborations are described in Section 3.1.

In the case of other types of production processes, such as electroweak production and strong-weak production, or in few cases where the sparticle masses fall outside the range previously described, the NLO approach is considered using PROSPINO2.

A special treatment is performed in scenarios in which either the squarks or the gluinos are set at a very large scale such that their production is not possible at the LHC. Defining this large scale is arbitrary and in some cases it may have a non-negligible impact in the production of the SUSY particles residing at the TeV scale (e.g. squarks at high scales can still contribute to the gluino pair production process via a t -channel exchange). Thus, instead of setting an explicit arbitrary value for the mass of the decoupled particle, the NLO+NLL calculation implemented in NLL-FAST assumes that this production does not interfere in any possible way with the production processes of the rest of the particles. Thus, the particle is completely decoupled from the rest of the phenomenology at the TeV scale.

The uncertainties due to the choice of the renormalisation and factorisation scales as well as the PDF are obtained using the NLL-FAST code or computed with PROSPINO2. In order to combine all these predictions and obtain an overall uncertainty, the PDF4LHC recommendations are followed as close as possible, subject to the current availability of the different calculations. Thus, an envelope of cross section predictions is defined using the 68% C.L. ranges of the CTEQ6.6 [26] (including the α_s uncertainty) and MSTW2008 [27] PDF sets, together with the variations of the scales. The nominal cross section is obtained using the midpoint of the envelope and the uncertainty assigned is half the full width of the envelope. Mathematically, if $\text{PDF}_{\text{CTEQ,up}}$ ($\text{PDF}_{\text{CTEQ,down}}$) and $\text{SCA}_{\text{CTEQ,up}}$ ($\text{SCA}_{\text{CTEQ,down}}$) are the upwards (downwards) one sigma variations of the CTEQ6.6 PDF set, respectively, $\text{PDF}_{\text{MSTW,up}}$ ($\text{PDF}_{\text{MSTW,down}}$) and $\text{SCA}_{\text{MSTW,up}}$ ($\text{SCA}_{\text{MSTW,down}}$) are the corresponding variations for the MSTW2008 PDF set and, finally, $\alpha_{s,\text{up}}$ ($\alpha_{s,\text{down}}$) is the corresponding up (down) one sigma uncertainty of the α_s coupling constant, the following quantities can be calculated:

$$\text{CTEQ}_{\text{up}} = \sqrt{\text{PDF}_{\text{CTEQ,up}}^2 + \text{SCA}_{\text{CTEQ,up}}^2 + \alpha_{s,\text{up}}^2}, \quad (7a)$$

$$\text{CTEQ}_{\text{down}} = \sqrt{\text{PDF}_{\text{CTEQ,down}}^2 + \text{SCA}_{\text{CTEQ,down}}^2 + \alpha_{s,\text{down}}^2}, \quad (7b)$$

$$\text{MSTW}_{\text{up}} = \sqrt{\text{PDF}_{\text{MSTW,up}}^2 + \text{SCA}_{\text{MSTW,up}}^2}, \quad (7c)$$

$$\text{MSTW}_{\text{down}} = \sqrt{\text{PDF}_{\text{MSTW,down}}^2 + \text{SCA}_{\text{MSTW,down}}^2}. \quad (7d)$$

The corresponding upper and lower values of the envelope created by this set of numbers and the nominal predictions (CTEQ_{nom} and MSTW_{nom}) is obtained by:

$$U = \max(\text{CTEQ}_{\text{nom}} + \text{CTEQ}_{\text{up}}, \text{MSTW}_{\text{nom}} + \text{MSTW}_{\text{up}}), \quad (8a)$$

$$L = \min(\text{CTEQ}_{\text{nom}} - \text{CTEQ}_{\text{down}}, \text{MSTW}_{\text{nom}} - \text{MSTW}_{\text{down}}), \quad (8b)$$

and the final corresponding cross section (σ) and its symmetric uncertainty ($\Delta\sigma$) is taken to be:

$$\sigma = (U + L)/2, \tag{9a}$$

$$\Delta\sigma = (U - L)/2. \tag{9b}$$

Full compliance with the PDF4LHC recommendations, with the inclusion of other PDF sets such as NNPDF [60], will be implemented in the near future. We notice that, as discussed in section 4, the additional contribution to the systematics coming from α_s uncertainties is negligible.

3.1 Special cases

Some models require special treatment in order to make sure that the NLO cross sections are correctly computed. This is important because of the way higher order calculations handle different squark flavours, which could lead to double-counting of diagrams. Given the difficulty to provide a comprehensive summary of all situations that are being considered in the interpretation of the LHC data, we only discuss here few relevant cases, to exemplify the approach followed.

Simplified Models

A variety of simplified models [61] are considered by the experiments. In some cases, the gluino, sbottom, and stop squarks are decoupled from the rest of the supersymmetric spectrum.²⁾ In this specific simplified model, only squark-antisquark production is allowed and this process is flavour-blind, if the masses are considered degenerate. Since the NLO+NLL calculations consider the sbottom as degenerate in mass with the squarks of the first and second generations, the overall cross section has to be rescaled down by a factor of $4/5 = 0.8$.

In other cases where the gluino is not decoupled, squark-gluino and squark-squark productions are feasible and they are not corrected further. The only effect could come from a b -quark in the initial state, which is suppressed [23]. Other types of simplified models decouple not only the squarks from the third generation particles, but also all the right-handed squarks. These scenarios primarily focus on final state decays via charginos or neutralinos. The squark mass is calculated by averaging the non-decoupled squark masses and the final cross section is rescaled down by a factor of $(4/5) \cdot (1/2) = 0.4$.

Treatment of 3rd generation squarks

Direct stop and sbottom production must be treated differently from the rest of squark families because, for instance, the t -channel gluino-exchange diagrams are suppressed. In beyond the leading-order computations processes involving sbottoms can be degenerate with the rest of the other squark flavours, this could lead to a potential double counting of sub-processes. In order to avoid this, in scenarios in which the production of different squark flavours are present, the squark pair production cross section is rescaled down to subtract the sbottom contribution and the corresponding process is computed separately.

At leading order the production cross sections for the third-generation squarks depend only on their masses, and the results for sbottom and stop of the same mass are therefore equal. At NLO in SUSY-QCD, additional SUSY parameters like squark and gluino masses or the stop/sbottom mixing angle enter. Their numerical impact, however, is very small [15, 23]. A further difference between stop and sbottom pair production arises from the $b\bar{b} \rightarrow \tilde{b}\tilde{b}^*$ channel, where the initial-state bottom quarks do allow a t -channel gluino-exchange graph that gives rise to extra contributions. However, as has been demonstrated in Ref. [23] their numerical impact on the hadronic cross sections is negligible. Thus, for all practical purposes, the LO and higher-order cross-section predictions obtained for stop-pair production apply also to sbottom-pair production if the input parameters, i.e. masses and mixing angles, are modified accordingly.

4 Gluino and squark production at the LHC

The production cross sections and associated uncertainties resulting from the procedure described in the previous section are discussed here for different processes of interest. We discuss three distinct cases: gluino pair production

²⁾ While this scenario is possible if we only consider the TeV scale, it bears some challenges at higher energy scales. Any kind of renormalisation scale evolution will generate squark masses at the scale of the gluino mass, but not vice versa. Thus, any discovery of light squarks associated with heavy gluinos would point to a non-standard underlying model [62]. In spite of all theory prejudice it is clearly adequate that these regions be experimentally explored.

with squarks decoupled, squark-antisquark pair production with gluino decoupled and stop/sbottom pair production. The results shown here are mainly illustrative: tables with cross sections and systematics obtained in other scenarios which take into account the full complexity of the spectrum, as a function of the parameters of various SUSY models, are collected at the SUSY cross section working group twiki page [7].

4.1 Gluino pair production

The gluino pair production cross section in a model where the squarks are decoupled is shown in Figure 1, for a gluino mass range spanning the current sensitivity of the ATLAS and CMS experiments. In the figure, the black (red) line corresponds to the NLO+NLL nominal cross section and renormalisation and factorisation scale uncertainties obtained using the CTEQ6.6 (MSTW2008) PDF set. The solid yellow (dashed black) band corresponds to the total uncertainty of the cross section using CTEQ6.6 (MSTW2008), as derived from Eq. 7a. Finally, the green solid lines delimit the envelope and the central value. They correspond to the central nominal value along with the total uncertainties.

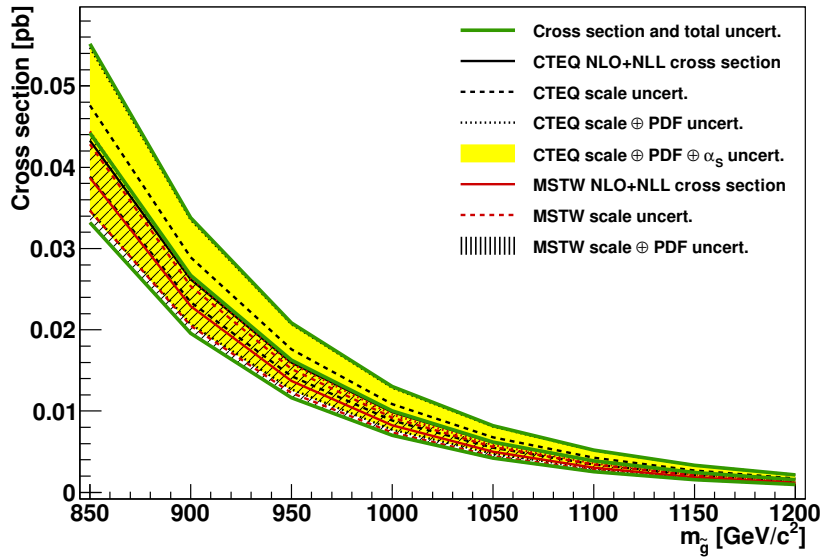


Figure 1: NLO+NLL gluino pair production cross section with squarks decoupled as a function of mass. The different styled black (red) lines correspond to the cross section and scale uncertainties predicted using the CTEQ6.6 (MSTW2008) PDF set. The yellow (dashed black) band corresponds to the total CTEQ6.6 (MSTW2008) uncertainty, as described in the text. The green lines show the final cross section and its total uncertainty.

As it can be seen, the cross sections predicted using the MSTW2008 PDF set are lower than the ones predicted by CTEQ6.6. For this mass range the uncertainty using MSTW2008 is approximately half that of the CTEQ6.6 set. Thus, the impact of the MSTW2008 prediction in the current prescription is almost negligible. The small difference between the green and black dotted lines also shows that the impact of the α_s uncertainty in the CTEQ6.6 case is negligible. This is consistent with the intuition that at the large values of x that are relevant for SUSY particle production, the intrinsic PDF uncertainty dominates over the small evolution differences caused at these high scales by the α_s uncertainty. This justifies as a good approximation not including the α_s uncertainty in the MSTW2008 case.

4.2 Squark-antisquark production

In order to show the evolution of the squark-antisquark production cross section as a function of the squark mass, a scenario has been chosen in which the gluino is decoupled. The results are shown in Figure 2, using the same graphical convention described in the gluino pair production case. The central values predicted using the CTEQ6.6 and MSTW2008 PDF sets are relatively close to each other. Again, the MSTW2008 uncertainty is the smallest of the two, although relatively larger than in case of gluino pair production.

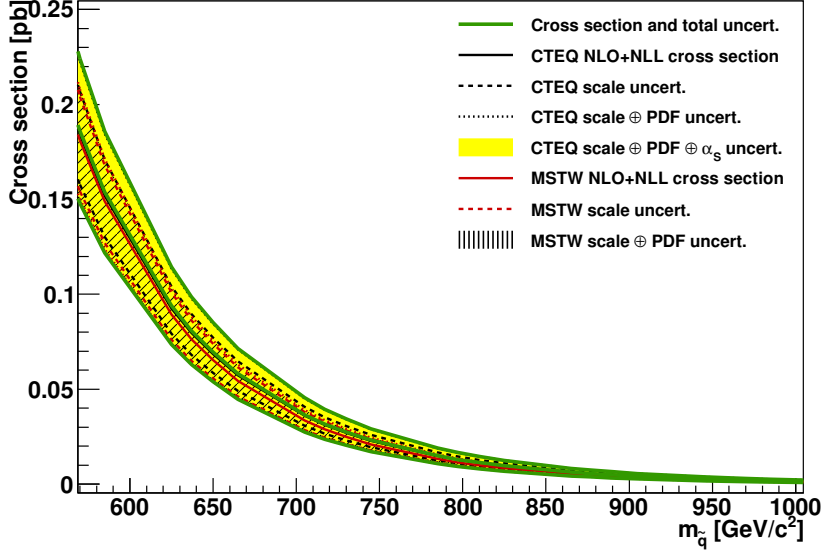


Figure 2: NLO+NLL squark-antisquark production cross section with gluinos decoupled as a function of mass. The different styled black (red) lines correspond to the cross section and scale uncertainties predicted using the CTEQ6.6 (MSTW2008) PDF set. The yellow (dashed black) band corresponds to the total CTEQ6.6 (MSTW2008) uncertainty, as described in the text. The green lines show the final cross section and its total uncertainty.

4.3 Direct stop and sbottom productions

The production cross section as a function of the stop mass for a model in which only the lightest stop is reachable by the LHC is shown in Figure 3. It should be noted that these cross sections are the same to those of a model in which only the lightest sbottom is accessible, assuming the rest of the coloured SUSY spectrum decoupled.

We discuss two different cases depending on the stop mass. For low stop masses, the cross sections predictions using the MSTW2008 PDF set are larger than the ones using CTEQ6.6, but the relative uncertainties are similar. Thus, the total cross section and the overall uncertainty are larger than those predicted by CTEQ6.6 alone. For larger stop mass ranges, the predictions using any of the two PDF sets under consideration are quite similar for the central value and its associated uncertainties. The final prediction is mostly determined by the CTEQ6.6 PDF set.

5 SUSY electroweak production at the LHC

SUSY electroweak particles are usually produced via cascade decays but they can also be directly produced. In this section we study the production cross sections along with the theoretical uncertainties using a CMSSM [63] scenario with $\tan\beta = 10$, $A_0 = 0$ GeV and $\mu > 0$. Figure 4 shows the NLO cross section for various SUSY electroweak productions in the $m_0 - m_{1/2}$ mass plane. The pure electroweak states have much lower cross sections in comparison with SUSY colour production. All possible combinations of charginos/neutralinos ($\tilde{\chi}$) and sleptons (\tilde{l}) are considered for the rate given by $\tilde{\chi}\tilde{\chi}$ and $\tilde{l}\tilde{l}$ sub-processes, respectively. The theoretical uncertainty due to the scale variation is found to be less than 10% for pure electroweak states as shown in Figure 5. The squark and electroweak gaugino associated sub-processes can have errors as large as 35%. The systematics due to the CTEQ6.6 and MSTW2008 PDFs for $\tilde{\chi}\tilde{\chi}$ are found to be less than 5%. The uncertainties on the rest of the sub-processes, as shown in Figure 6 and Figure 7, are negligible.

6 Summary and future prospects

We presented here a proposal ³⁾, based on state-of-the-art higher-order calculations, for the definition of benchmark production cross sections and associated theoretical uncertainties of various SUSY processes of interest at the

³⁾ This documentation should be cited along with the original papers, i.e. Refs. [14, 20, 21, 22, 24] for inclusive squark/gluino production, Refs. [15, 23, 24] for stop or sbottom direct production, and Ref. [57] for the production of electroweak gauginos.

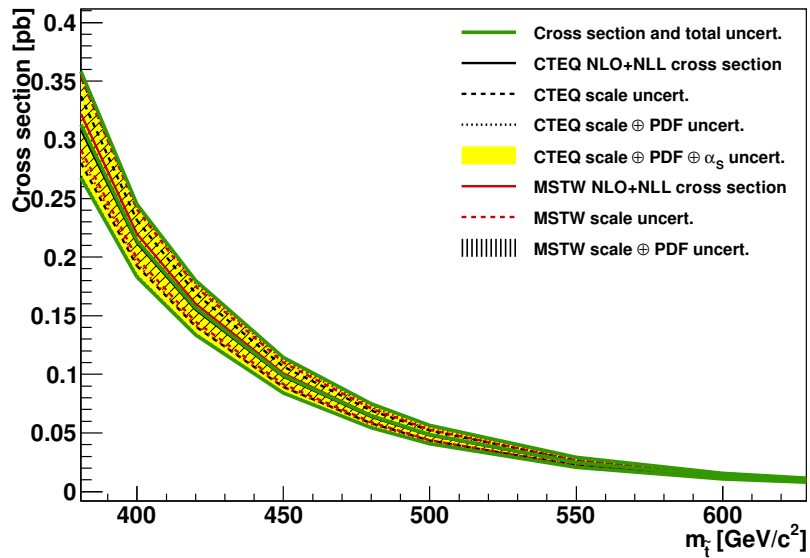
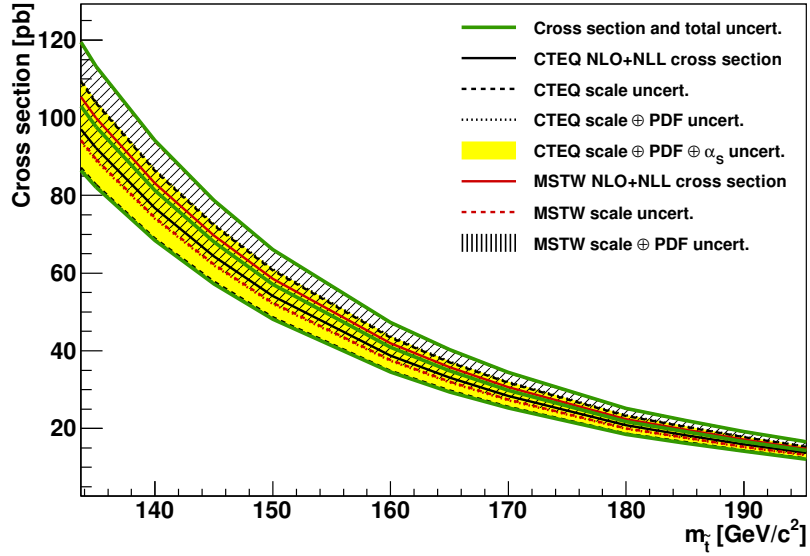


Figure 3: NLO+NLL stop-antistop production cross section as a function of mass. The different styled black (red) lines correspond to the cross section and scale uncertainties predicted using the CTEQ6.6 (MSTW2008) PDF set. The yellow (dashed black) band corresponds to the total CTEQ6.6 (MSTW2008) uncertainty, as described in the text. The green lines show the final cross section and its total uncertainty. The figure on the top (bottom) shows a low (high) stop mass range.

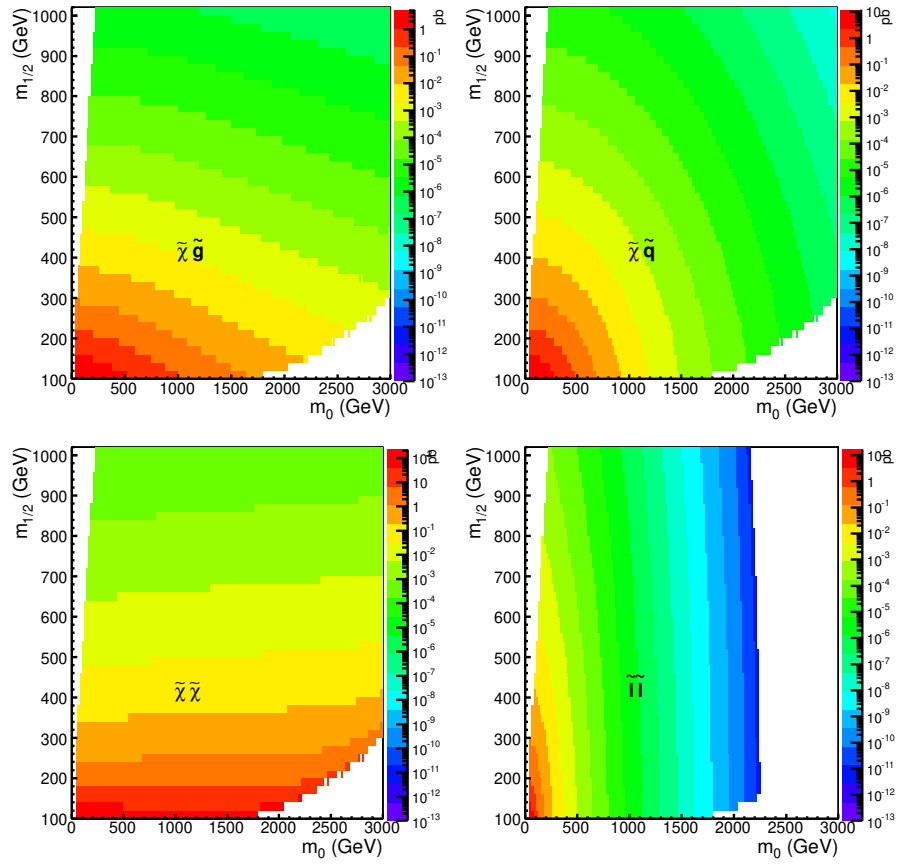


Figure 4: NLO cross sections for SUSY electroweak productions in the $m_0 - m_{1/2}$ plane using CTEQ6.6 PDF set. The CMSSM framework is used, with $\tan \beta = 10$, $A_0 = 0$ GeV and $\mu > 0$.

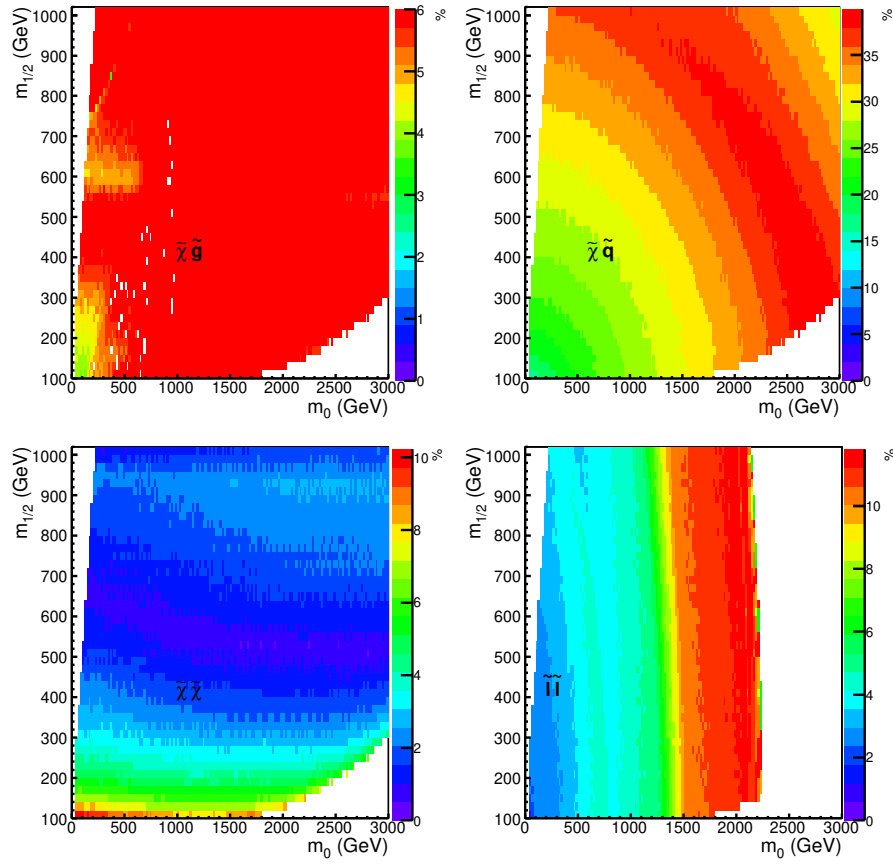


Figure 5: Uncertainties in percentage due to the scale choice for SUSY electroweak productions in the $m_0 - m_{1/2}$ plane using CTEQ6.6 PDF set. The CMSSM framework is used, with $\tan \beta = 10$, $A_0 = 0$ GeV and $\mu > 0$.

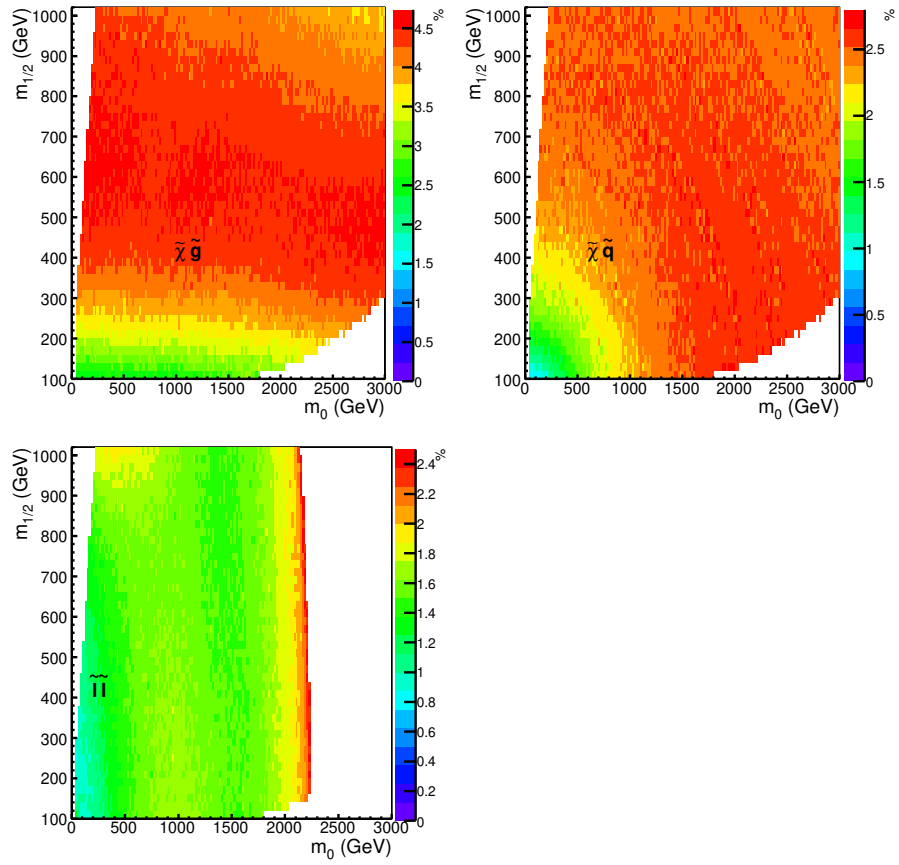


Figure 6: Uncertainties in percentage due to CTEQ6.6 PDF error prescription for SUSY electroweak productions in the $m_0 - m_{1/2}$ plane. The CMSSM framework is used with $\tan \beta = 10$, $A_0 = 0$ GeV and $\mu > 0$.

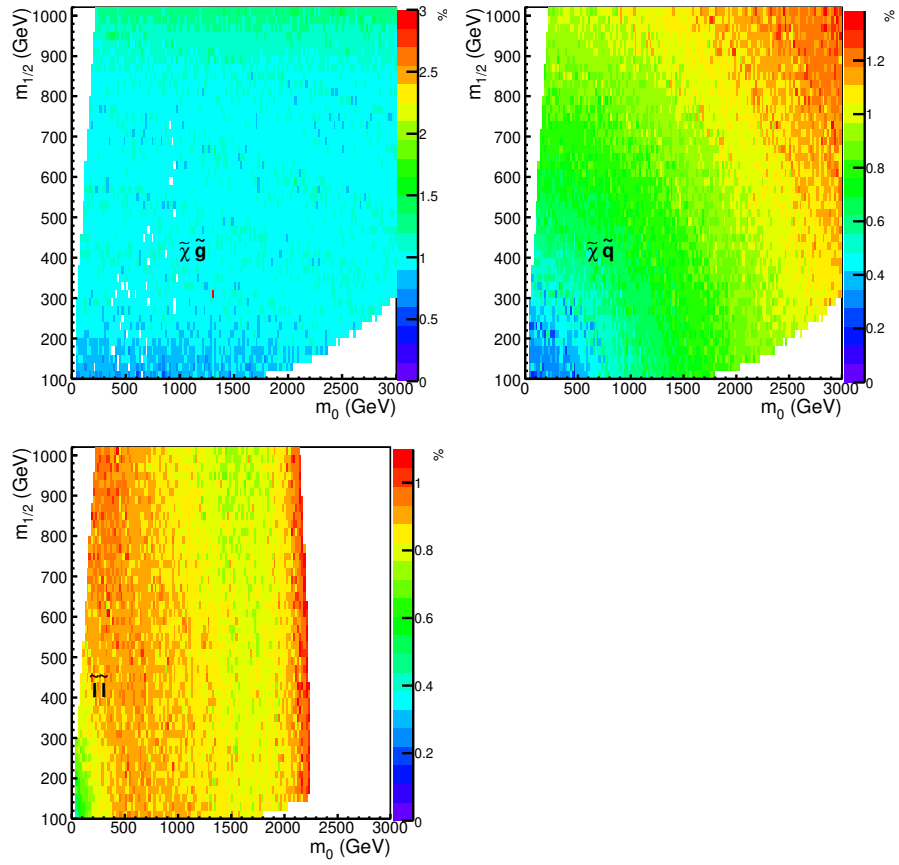


Figure 7: Uncertainties in % due to MSTW2008 PDF error prescription for SUSY electroweak productions in the $m_0 - m_{1/2}$ plane. The CMSSM framework is used, with $\tan \beta = 10$, $A_0 = 0$ GeV and $\mu > 0$.

LHC. The common set of prescriptions described in this document aims to establish a reference framework for the theoretical input used by the ATLAS and CMS collaborations in the interpretation of their measurements.

We presented a collection of explicit results for collisions at a centre-of-mass energy of 7 TeV. The theoretical systematic uncertainties are larger for higher masses, and they are typically dominated by the PDF uncertainties. These have a significant impact when assessing the experimental constraints or the sensitivity to a given SUSY model. Detailed numbers and tables for a broad class of SUSY models and parameters are collected at the SUSY cross section working group twiki page [7], where the results corresponding to higher collision energies will also appear soon.

The LHC has recently raised the centre-of-mass energy and the experiments are already analysing data from these collisions. Hence, the current set of prescriptions will evolve and is expected to adapt to 8 TeV collisions. In particular, the mass ranges for which the NLO+NLL calculations are available will be enlarged including usage of the complete PDF4LHC prescription.

Acknowledgements

We would like to thank W. Beenakker, S. Brensing, R. Höpker, M. Klasen, E. Laenen, L. Motyka, I. Niessen, M. Spira and P.M. Zerwas for a fruitful collaboration on SUSY cross section calculations. This work has been supported by the Helmholtz Alliance “Physics at the Terascale”, the DFG SFB/TR9 “Computational Particle Physics”, the Foundation for Fundamental Research of Matter (FOM), the Netherlands Organisation for Scientific Research (NWO), the Polish National Science Centre grant, project number DEC-2011/01/B/ST2/03643, and the ERC grant 291377 “LHCtheory”. MK thanks the CERN TH unit for hospitality. SP acknowledges support from the DOE under the grant DOE -FG02-90ER40546.

References

- [1] <https://twiki.cern.ch/twiki/bin/view/AtlasPublic/SupersymmetryPublicResults>
- [2] <https://twiki.cern.ch/twiki/bin/view/CMSPublic/PhysicsResultsSUS>
- [3] <http://cern.ch/lpcc>
- [4] M. Botje, J. Butterworth, A. Cooper-Sarkar, A. de Roeck, J. Feltesse, et al., arXiv:1101.0538 [hep-ph].
- [5] S. Dittmaier *et al.* [LHC Higgs Cross Section Working Group Collaboration], arXiv:1101.0593 [hep-ph].
- [6] S. Dittmaier, S. Dittmaier, C. Mariotti, G. Passarino, R. Tanaka, S. Alekhin, J. Alwall and E. A. Bagnaschi *et al.*, arXiv:1201.3084 [hep-ph].
- [7] <https://twiki.cern.ch/twiki/bin/view/LHCPhysics/SUSYCrossSections>
- [8] G. L. Kane and J. P. Leveille, *Phys. Lett. B* **112**, (1982) 227.
- [9] P. R. Harrison and C. H. Llewellyn Smith, *Nucl. Phys. B* **213**, (1983) 223, [*Erratum-ibid. B* **223**, (1983) 542].
- [10] S. Dawson, E. Eichten and C. Quigg, *Phys. Rev. D* **31**, (1985) 1581.
- [11] W. Beenakker, S. Brensing, M. D’Onofrio, M. Krämer, A. Kulesza, E. Laenen, M. Martinez and I. Niessen, arXiv:1106.5647 [hep-ph].
- [12] W. Beenakker, R. Höpker, M. Spira and P. M. Zerwas, *Phys. Rev. Lett.* **74**, (1995) 2905, [arXiv:hep-ph/9412272].
- [13] W. Beenakker, R. Höpker, M. Spira and P. M. Zerwas, *Z. Phys. C* **69**, (1995) 163, [arXiv:hep-ph/9505416].
- [14] W. Beenakker, R. Höpker, M. Spira and P. M. Zerwas, *Nucl. Phys. B* **492**, (1997) 51, [arXiv:hep-ph/9610490].
- [15] W. Beenakker, M. Krämer, T. Plehn, M. Spira and P. M. Zerwas, *Nucl. Phys. B* **515**, (1998) 3, [arXiv:hep-ph/9710451].
- [16] publicly available from www.thphys.uni-heidelberg.de/~plehn

- [17] T. Binoth, D. Goncalves Netto, D. Lopez-Val, K. Mawatari, T. Plehn and I. Wigmore, *Phys. Rev. D* **84** (2011) 075005, [arXiv:1108.1250 [hep-ph]].
- [18] J. Alwall, P. Demin, S. de Visscher, R. Frederix, M. Herquet, F. Maltoni, T. Plehn and D. L. Rainwater *et al.*, *JHEP* **0709** (2007) 028, [arXiv:0706.2334 [hep-ph]].
- [19] C. Weydert, S. Frixione, M. Herquet, M. Klasen, E. Laenen, T. Plehn, G. Stavenga and C. D. White, *Eur. Phys. J. C* **67** (2010) 617 [arXiv:0912.3430 [hep-ph]].
- [20] A. Kulesza and L. Motyka, *Phys. Rev. Lett.* **102**, (2009) 111802, [arXiv:0807.2405 [hep-ph]].
- [21] A. Kulesza and L. Motyka, *Phys. Rev. D* **80**, (2009) 095004 [arXiv:0905.4749 [hep-ph]].
- [22] W. Beenakker, S. Brensing, M. Krämer, A. Kulesza, E. Laenen and I. Niessen, *JHEP* **0912**, (2009) 041 [arXiv:0909.4418 [hep-ph]].
- [23] W. Beenakker, S. Brensing, M. Krämer, A. Kulesza, E. Laenen and I. Niessen, *JHEP* **1008**, (2010) 098 [arXiv:1006.4771 [hep-ph]].
- [24] W. Beenakker, S. Brensing, M. Krämer, A. Kulesza, E. Laenen, L. Motyka and I. Niessen, *Int. J. Mod. Phys. A* **26** (2011) 2637 [arXiv:1105.1110 [hep-ph]].
- [25] S. Catani, M. L. Mangano, P. Nason and L. Trentadue, *Nucl. Phys. B* **478** (1996) 273 [arXiv:hep-ph/9604351].
- [26] Pavel M. Nadolsky *et. al*, *Phys. Rev. D* **78** (2008) 013004.
- [27] A.D. Martin, W.J. Stirling, R.S. Thorne, G. Watt, *Eur. Phys. J. C* **63** (2009) 189.
- [28] G. F. Sterman and W. Vogelsang, hep-ph/0002132.
- [29] Publicly available from [7]
- [30] W. Beenakker, S. Brensing, M. Krämer, A. Kulesza, E. Laenen and I. Niessen, *JHEP* **1201** (2012) 076 [arXiv:1110.2446 [hep-ph]].
- [31] M. Beneke, P. Falgari and C. Schwinn, *Nucl. Phys. B* **828**, 69 (2010) [arXiv:0907.1443 [hep-ph]].
- [32] M. Beneke, P. Falgari, C. Schwinn, *Nucl. Phys. B* **842**, 414-474 (2011). [arXiv:1007.5414 [hep-ph]].
- [33] P. Falgari, C. Schwinn and C. Wever, arXiv:1202.2260 [hep-ph].
- [34] U. Langenfeld and S. O. Moch, *Phys. Lett. B* **675**, 210 (2009) [arXiv:0901.0802 [hep-ph]].
- [35] U. Langenfeld, [arXiv:1011.3341 [hep-ph]].
- [36] K. Hagiwara and H. Yokoya, *JHEP* **0910**, 049 (2009) [arXiv:0909.3204 [hep-ph]].
- [37] M. R. Kauth, J. H. Kuhn, P. Marquard, M. Steinhauser, *Nucl. Phys.* **B831** (2010) 285-305 [arXiv:0910.2612 [hep-ph]].
- [38] M. R. Kauth, J. H. Kuhn, P. Marquard and M. Steinhauser, *Nucl. Phys. B* **857** (2012) 28 [arXiv:1108.0361 [hep-ph]].
- [39] M. R. Kauth, A. Kress and J. H. Kuhn, *JHEP* **1112** (2011) 104 [arXiv:1108.0542 [hep-ph]].
- [40] W. Hollik, M. Kollar and M. K. Trenkel, *JHEP* **0802**, 018 (2008) [arXiv:0712.0287 [hep-ph]].
- [41] W. Hollik and E. Mirabella, *JHEP* **0812**, 087 (2008) [arXiv:0806.1433 [hep-ph]].
- [42] W. Hollik, E. Mirabella and M. K. Trenkel, *JHEP* **0902**, 002 (2009) [arXiv:0810.1044 [hep-ph]].
- [43] M. Beccaria, G. Macorini, L. Panizzi, F. M. Renard and C. Verzegnassi, *Int. J. Mod. Phys. A* **23**, 4779 (2008) [arXiv:0804.1252 [hep-ph]].
- [44] E. Mirabella, *JHEP* **0912**, 012 (2009) [arXiv:0908.3318 [hep-ph]].
- [45] J. Germer, W. Hollik, E. Mirabella, M. K. Trenkel, *JHEP* **1008** (2010) 023. [arXiv:1004.2621 [hep-ph]].

- [46] J. Germer, W. Hollik, E. Mirabella, [arXiv:1103.1258 [hep-ph]].
- [47] A. T. Alan, K. Cankocak and D. A. Demir, *Phys. Rev. D* **75**, 095002 (2007) [*Erratum-ibid. D* **76**, 119903 (2007)] [arXiv:hep-ph/0702289].
- [48] S. Bornhauser, M. Drees, H. K. Dreiner and J. S. Kim, *Phys. Rev. D* **76**, 095020 (2007) [arXiv:0709.2544 [hep-ph]].
- [49] G. Bozzi, B. Fuks and M. Klasen, *Phys. Rev. D* **74** (2006) 015001 [hep-ph/0603074].
- [50] G. Bozzi, B. Fuks and M. Klasen, *Nucl. Phys. B* **777** (2007) 157 [hep-ph/0701202].
- [51] C. S. Li, Z. Li, R. J. Oakes and L. L. Yang, *Phys. Rev. D* **77** (2008) 034010 [arXiv:0707.3952 [hep-ph]].
- [52] G. Bozzi, B. Fuks and M. Klasen, *Nucl. Phys. B* **794** (2008) 46 [arXiv:0709.3057 [hep-ph]].
- [53] J. Debove, B. Fuks and M. Klasen, *Phys. Lett. B* **688** (2010) 208 [arXiv:0907.1105 [hep-ph]].
- [54] J. Debove, B. Fuks and M. Klasen, *Nucl. Phys. B* **842** (2011) 51 [arXiv:1005.2909 [hep-ph]].
- [55] J. Debove, B. Fuks and M. Klasen, *Nucl. Phys. B* **849** (2011) 64 [arXiv:1102.4422 [hep-ph]].
- [56] A. Broggio, M. Neubert and L. Vernazza, *JHEP* **1205** (2012) 151 [arXiv:1111.6624 [hep-ph]].
- [57] W. Beenakker, M. Klasen, M. Krämer, T. Plehn, M. Spira and P. M. Zerwas, *Phys. Rev. Lett.* **83** (1999) 3780 [*Erratum-ibid.* **100** (2008) 029901] [hep-ph/9906298].
- [58] E. L. Berger, M. Klasen and T. M. P. Tait, *Phys. Rev. D* **62** (2000) 095014 [hep-ph/0005196] [*Erratum-ibid.* **67** (2003) 099901 [hep-ph/0212306]].
- [59] M. Spira, hep-ph/0211145.
- [60] F. Demartin et al., *Phys. Rev. D* **82** (2010) 014002
- [61] D. Alves et. al, [arXiv:1105.2838 [hep-ph]].
- [62] J. Jaeckel, V. V. Khoze, T. Plehn and P. Richardson, *Phys. Rev. D* **85** (2012) 015015, [arXiv:1109.2072 [hep-ph]].
- [63] G.L. Kane et. al., *Phys. Rev. D* **49** (1994) 6173, [hep-ph/9312272];
for a recent discussion of SUSY benchmark scenarios see S. S. AbdusSalam, B. C. Allanach, H. K. Dreiner, J. Ellis, U. Ellwanger, J. Gunion, S. Heinemeyer and M. Krämer *et al.*, *Eur. Phys. J. C* **71** (2011) 1835 [arXiv:1109.3859 [hep-ph]].